Mutagenesis of the H-*ras* p21 at Glycine-60 Residue Disrupts GTP-Induced Conformational Change†

Ying-Ju Sung,‡,§ Mary Carter,‡,|| Jie-Ming Zhong,‡ and Yu-Wen Hwang*,‡,§

Molecular Biology Department, New York State Institute for Basic Research in Developmental Disabilities, 1050 Forest Hill Road, Staten Island, New York 10314, and CSI/IBR Center for Developmental Neuroscience and Graduate Program in Biology, City University of New York, New York, New York 10021

Received October 6, 1994; Revised Manuscript Received December 21, 1994⊗

ABSTRACT: The function of Gly-60, the conserved glycine in the DXXG domain of v-H-*ras*, was examined by site-directed mutagenesis. It was found that while the G60A (Gly-60 to Ala substitution) mutation has little effect on the interaction of H-*ras* with guanine nucleotides, it completely abolishes the biological activity of v-H-*ras*. The G60A mutation also exerts little effect on the interaction of H-*ras* with SDC25C (a guanine nucleotide exchange factor) and GAP. However, the G60A mutation does lower the ability of H-*ras* to bind Raf. GTP induces an enhancement of fluorescence emission in complexes consisting of H-*ras* and the fluorescent dye 8-anilino-1-naphthalenesulfonic acid. This enhancement is blocked by the G60A mutation. On the basis of these observations, we propose that the GTP-induced conformational change of H-*ras*, a process required for H-*ras* activities, is impaired by the G60A mutation.

Gly-60 of Ras p21 is located in the conserved DXXG domain of regulatory GTPases (Dever *et al.*, 1987). This domain together with other conserved sequences, such as GXXXXGKS/T and NKXD, form the GDP/GTP binding pocket in regulatory GTPases (Bourne *et al.*, 1990, 1991). In addition to GDP/GTP binding, these residues may serve as the foundation for various conserved molecular mechanisms of regulatory GTPases, which include GTP-induced conformational changes, GTP hydrolysis, and guanine nucleotide exchange (Bourne *et al.*, 1990, 1991).

DXXG motif forms a sharp flexible turn (loop 4) connecting β-strand 3 and α-helix 2 of H-*ras* p21 (De Vos *et al.*, 1988; Pai *et al.*, 1989). This sharp turn requires a Gly residue because Gly exhibits a much broader range of ϕ and ψ dihedral angles than other amino acids (Richardson, 1981). The GTP-induced conformational change appears to originate at around residues 59−60 and then propagates to other regions of p21, primarily, residues 30−38 (loop 2, the effector region, switch I) and 60−76 (loop 4 and helix 2, switch II) (Pai *et al.*, 1989; Milburn *et al.*, 1990; Stouten *et al.*, 1993). These conformational changes not only involve the movement of protein domains, but also include a massive reorientation, particularly, in loop 4. This reorientation redirects the amide group of Gly-60 from a residue in helix 2 (possibly Glu-63) to the γ-phosphate of GTP. This subsequently forces part of helix 2 to relax into an extended loop 4 and to rotate along its own helix axis. Presumably, these changes help to place helix 2 and loop 2 regions in favorable positions for target binding and GTP hydrolysis (Pai *et al.*, 1989; Milburn *et al.*, 1990; Stouten *et al.*, 1993). These results are consistent with the findings that loop 2 and helix 2 are important for interacting with GAP[1] and the Raf gene product, two putative targets of Ras p21, in a GTP-dependent manner (Bollag & McCormick, 1991; Marshall, 1993; Moodie *et al.*, 1993; Van Aslet *et al.*, 1993; Vojtek *et al.*, 1993; Warne *et al.*, 1993; Zhang *et al.*, 1993).

Although they possess only modest sequence similarities, the X-ray structures of H-*ras* p21 and the EF-Tu G-domain are nearly superimposable (Valencia *et al.*, 1991; Jurnak *et al.*, 1990); therefore, it is expected that GTP will induce similar conformational changes in both EF-Tu and H-*ras* p21. The corresponding Gly-60 residue of EF-Tu, Gly-83 of EF-Tu from *Escherichia coli* (Jurnak, 1985; la Cour *et al.*, 1985) and Gly-84 of EF-Tu from *Thermus thermophilus* (Berchtold *et al.*, 1993) and *Thermus aquaticus* (Kjeldgaard *et al.*, 1993), appears to assume the same role as the Gly-60 of H-*ras* p21. This residue reorients in response to GTP and initiates molecular rearrangements parallel to those of H-*ras* p21. The conformational change subsequently extends to other domains of EF-Tu and renders the protein capable of binding aminoacyl-tRNA and ribosomes (Berchtold *et al.*, 1993; Kjeldgaard *et al.*, 1993). Despite the nature of the GTP-induced conformational change of heterotrimeric G-protein is inherently more complex than that of H-*ras* (and EF-Tu) and many of the details are different, the basic mechanism appears to be similar. That is, the conserved glycine (Gly-199 in α subunit of transducin), again, plays a pivotal role

† This work was supported in part by New York State Office of Mental Retardation and Developmental Disabilities, and by NIH Grants CA53782. Y.-J.S. was supported by a fellowship from New York State Office of Mental Retardation and Developmental Disabilities.

* To whom correspondence should be addressed at the Molecular Biology Department, New York State Institute for Basic Research in Developmental Disabilities, 1050 Forest Hill Rd., Staten Island, NY 10314. Tel: 718-494-5337; Fax: 718-494-5287.

‡ New York State Institute for Basic Research in Developmental Disabilities.

§ City University of New York.

|| Present address: PharmaGenics, Inc., 4 Pearl Ct., Allendale, NJ 07401.

⊗ Abstract published in *Advance ACS Abstracts,* February 15, 1995.

[1] Abbreviations: ANS, 8-anilino-1-naphthalenesulfonate; EF-Ts, elongation factor Ts; EF-Tu, elongation factor Tu; G60A, Gly-60 to Ala mutation; G83A, Gly-83 to Ala mutation; G226A, Gly-226 to Ala mutation; GAP, GTPase activating protein; GST, glutathione *S*-transferase; GVBD, germinal vesicle breakdown; c-H-*ras*, cellular H-*ras*; v-H-*ras*, viral H-*ras*; PCR, polymerase chain reaction; SDC25C, C-domain gene product of SDC25.

0006-2960/95/0434-3470$09.00/0

in the GTP-induced conformational change (Noel *et al.*, 1993; Lambright *et al.*, 1994).

The importance of this conserved Gly residue has been examined in $G_{s\alpha}$ and *E. coli* EF-Tu by substituting the invariant glycine with alanine, a change that should drastically reduce the ability to rearrange around the Gly residue. In $G_{s\alpha}$, mutation G226A does not appear to affect the strength of GDP/GTP binding nor does it affect the interaction of $G_{s\alpha}$ with its receptor (Miller *et al.*, 1988; Lee *et al.*, 1992). However, the mutation does block GTP-induced subunit dissociation and prevents the activation of adenylyl cyclase (Miller *et al.*, 1988; Lee *et al.*, 1992). The dissociation of α from $\beta\gamma$ subunits is known to be the essential step preceding adenylyl cyclase activation (Gilman, 1987). This observation has been interpreted as indicating that $G_{s\alpha}$-(G226A) has lost its ability to switch into its active form in the GTP-bound state. The G83A mutation in EF-Tu, the counterpart of $G_{s\alpha}$(G226A), affects EF-Tu similarly: abolishing GTP-induced aminoacyl-tRNA binding while not affecting EF-Tu's ability to bind GDP/GTP and EF-Ts (EF-Tu's specific guanine nucleotide exchange factor) (Hwang *et al.*, 1989). We constructed the Gly-60 to Ala substitution, the mutation corresponding to $G_{s\alpha}$(G226A) and EF-Tu-(G83A), and studied its effects on the functions of v-H-*ras*. Here, we describe its properties.

MATERIALS AND METHODS

Mutant Construction and Protein Purification. The G60A mutant was constructed by oligonucleotide site-directed mutagenesis as described by Kunkel and co-workers (Kunkel *et al.*, 1987). Single-stranded DNA from M13 phage clone containing the entire c-H-*ras* was used as the template for mutagenesis. The following mutagenic primer, CTTCT-TGAGCTGCTGTG, was used for mutant construction. Subsequently, the *H-ras* fragment was subcloned into vector pSV_{neo} and used for NIH3T3 cell transformation as previously described (Ogiso *et al.*, 1990). *E. coli* expression vectors, pHR for producing H-*ras* proteins under the control of the T7 RNA polymerase promoter, were constructed as described (Hwang *et al.*, 1993). These plasmids were converted to pA-H-*ras* clones by replacing the *Pst*1−*Hin*dIII-(2) fragment of pHR vector (Hwang *et al.*, 1993) with an oligonucleotide linker containing a *Sal*I site, 38 residues of poly(A) track, and a *Xho*I site, respectively. The resulting plasmid contains unique *Sal*I and *Xho*I sites 3′ to the H-*ras* coding sequence which can be used to produce run-off RNA. The procedures for H-*ras* protein induction and purification were described previously (Hwang *et al.*, 1993). SDC25C was expressed from the vector pTTQ-SDC25 (Mistou *et al.*, 1992) in an *E. coli* host and purified as described by Crechet *et al.* (1990).

Biological Assays. Transformation of NIH 3T3 cells was performed as previously described (Ogiso *et al.*, 1990), and foci were scored 2 weeks after transfection. Experiments involving *Xenopus* oocytes were performed as follows. Large *Xenopus laevis* females (10−12 cm) were obtained from Nasco (Fort Atkinson, WI). Frogs were injected with 35 units of chronic gonadotropin from pregnant mare's serum 3 days before the operation to accelerate oogenesis. Fragments of ovary were surgically removed from the frog anesthetized by low temperature. Fully developed stage VI oocytes (Dumont, 1972) were manually dissected and maintained in Barth's medium (Gurdon *et al.*, 1985). During isolation, most of the outer layer surrounding the oocytes (theca) was removed, but follicular cells remained essentially unaltered. The dissected oocytes were allowed to recover for at least 8 h at 19 °C before use. Proteins were diluted in a buffer (50 mM Tris-HCl, pH 7.4, 5 mM $MgCl_2$, and 1 mM DTT) and then injected (in a total volume of 46 nL) into the vegetal hemisphere of the cytoplasm using a nanoliter injector (Model A2033XVY, World Precision Instruments Inc.). Injected oocytes, usually in a group of 10−20 oocytes, were incubated at 19 °C, and GVBD was scored at various time points. GVBD was initially scored by the appearance of a white spot in the animal hemisphere and further confirmed by manual dissection of the oocytes fixed in 5% (w/v) trichloroacetic acid.

Guanine Nucleotide Binding, Exchange, and Dissociation. GDP/GTP dissociation constants were determined by equilibrium binding and calculated from Scatchard plots as described (Manne *et al.*, 1984). GTP/GDP exchange was performed by the following procedure. Two micrograms of purified p21 was incubated at 30 °C in 100 μL of exchange buffer containing 50 mM Tris-HCl, pH 7.5, 2 mM $MgCl_2$, 50 mM KCl, 10 mM 2-mercaptoethanol, 10 mg/mL bovine serum albumin, and 5 μM [^{3}H]GDP (sp act. 2 Ci/mmol) or [^{3}H]GTP (sp act. 2 Ci/mmol). The concentration of free Mg^{2+} in the reaction mixture was controlled by adding either EDTA or $MgCl_2$. At the indicated times, 20 μL aliquots of the reaction mixture were withdrawn and the radioactivity was determined by a nitrocellulose membrane binding assay (Miller & Weissbach, 1974). Percent of saturation was calculated by dividing the filter-bound radioactivity at the given time by the radioactivity obtained from the equilibrium binding. GTP/GDP dissociation experiments were performed by first labeling H-*ras* p21 with either [^{3}H]GDP (sp act. 2 Ci/mmol) or [^{3}H]GTP (sp act. 2 Ci/mmol) to equilibrium and then chasing with a 500-fold excess of cold guanine nucleotide. The SDC25C-stimulated guanine nucleotide exchange and kinetic parameters determination were performed as previously described (Hwang *et al.*, 1993).

In Vitro H-ras p21 Labeling and SDC25C Binding Assay. *In vitro* [^{35}S]-labeling of p21 and the SDC25C binding assay were performed exactly as described (Hwang *et al.*, 1993).

Measurement of GTPase Activity. The GAP competition assay was performed by monitoring the production of free phosphate as previously described (Vogel *et al.*, 1988) except that the isobutyl alcohol−benzene extraction method (Crystal *et al.*, 1974) was used instead of the charcoal-absorption method. Briefly, free phosphates in the reaction mixture were first converted to molybdate complexes by the addition of 0.3 mL of 1 mM potassium phosphate (pH 7.4) and 0.15 mL of 5% ammonium molybdate (dissolved in 4 N H_2SO_4). Subsequently, the molybdate−phosphate complex was extracted from the reaction mixture with 0.6 mL of isobutyl alcohol and benzene (1:1 mixture). The radioactivity in the organic phase was determined by a liquid scintillation counter and used to calculate the rate of GTP hydrolysis. The steady-state inhibition constant of GAP-stimulated GTP hydrolysis was determined as follows. Two sets of reaction mixture were set up, each with five different c-H-*ras*·[γ-^{32}P]GTP concentrations (1, 2, 3, 4, 5 μM) in a total volume of 30 μL containing 20 mM Na-Hepes, pH 7.5, 2 mM $MgCl_2$, and 2.8 nM GAP. One of the two sets included 50 μM inhibitor (either v-H-*ras*·GTP or v-H-*ras*(G60A)·GTP). Reactions

were initiated by the addition of GAP and were allowed to proceed for 5 min at 30 °C. The extent of GTP hydrolysis was determined by the isobutyl alcohol−benzene extraction method described above. Each data point was corrected for intrinsic GTPase activity before K_i calculation.

Preparation of GST-Raf Fusion Protein. The GST fusion protein containing the 275 residue N-terminal domain of Raf was constructed as follows. The N-terminal Raf domain DNA was prepared by PCR from a baculovirus expression clone containing the human full-length c-Raf gene (Bonner *et al.*, 1986). Oligos, TTCCTTATCGATGGAGCACATACAGGGAGCT and TTCCTTCTCGAGTCACATCCTGCTGTCCACAGGCAG, containing *Cla*I and *Xho*I sites, respectively, were used for PCR amplification. PCR produces a band of about 900 bps which was subsequently confirmed to be the human Raf gene by DNA sequencing. The PCR product was restricted by *Cla*I plus *Xho*I and then cloned into the unique *Cla*I−*Xho*I site of the modified pGEX3 vector (Pharmacia). The modification was done by inserting an oligonucleotide linker containing *Cla*I and *Xho*I cutting sites, CAATCGATGGCCGCCCTCGAGAATT, into the *Bam*HI−*Eco*RI site of pGEX3. GST-Raf fusion protein was expressed in *E. coli* strain MV1190 and purified as described below. All of the following procedures were performed at 4 °C. A bacterial pellet from a 1 L culture was resuspended in 20 mL of buffer G (1× PBS, pH 7.4, 1 mM DTT, 0.5 mM PMSF, and 1% Trition X-100) and sonicated 10 times (30 s, each sonication) with a Branson cell disrupter. Cell debris was removed by centrifugation at 12000*g* for 10 min. The resulting supernatant was incubated with 3 mL of PBS and buffer G-equilibrated glutathione−Sepharose 4B for 6 h. The resin was recovered by centrifugation at 2000*g* for 10 min and then washed with 60 mL of buffer G without Triton. The elution of GST-Raf from the resin was accomplished by incubating the protein-bound resin in 10 mL of elution buffer (10 mM glutathione in 50 mM Tris-HCl, pH8) for 2 h. The buffer containing GST-Raf protein was then switched to a buffer containing 50 mM Tris-HCl, pH 7.4, 150 mM NaCl, and 1 mM DTT using an Amicon Centriprep-10 concentrator. Purified protein was stored at −70 °C until use.

Raf and Ras Binding Assay. [^{35}S]-labeled H-*ras* p21 was labeled with guanine nucleotides (GDP or GTP) at 30 °C to equilibrium in a 35 μL binding solution containing 25 mM Tris, pH 7.5, 2 mM $MgCl_2$, 100 mM NH_4Cl, 0.2 mg/mL BSA, 0.5 mM GDP/or GTP, and 5 mM EDTA for 5 min. The reaction was terminated by the addition of 20 mM $MgCl_2$. Complex formation between Ras and Raf was determined by mixing the GDP or GTP equilibrated [^{35}S]-labeled Ras (5.6 pmol) with 2.8 nmol of GST-Raf fusion protein in 200 μL of Raf binding buffer composed of 50 mM Hepes, pH 7.5, 100 mM KCl, 20 μM $ZnCl_2$, 5 mM $MgCl_2$, and 1 mg/mL BSA. After incubating on ice for 1 h, 20 μL of glutathione−Sepharose beads (12.5% gel bed) was added to the reaction mixture and the incubation (with gentle shaking) was continued for another hour at 4 °C. The free Ras and GST-Raf were removed by washing the beads 5 times with 1 mL of ice-cold washing buffer (50 mM Hepes, pH 7.5, 100 mM KCl, 5 mM $MgCl_2$, 20 μM $ZnCl_2$, and 0.1% Triton X-100). Ras•GST-Raf complexes were then eluted from the washed beads by resuspending them in 30 μL of PAGE loading buffer. The amount of coprecipitated [^{35}S]-labeled Ras protein was analyzed by autoradiography following electrophoresis on a 10% Tricine−polyacrylamide gel. The quantitation of precipitated Ras was performed on a scanned image of the autoradiogram using IP Lab Gel, a image analysis program from Signal Analytics Corp. Alternatively, the complex formation was examined using Ras labeled with [γ-^{32}P]GTP as described by Chuang *et al.* (1994). Purified Ras was labeled with [γ-^{32}P]GTP (sp act. 4500 Ci/mmol) to equilibrium. The labeled Ras (2 pmol) was then allowed to react on ice with GST-Raf (2 nmol) for 1 h in 50 μL of Raf binding buffer. Subsequently, 20 μL of glutathione−Sepharose beads was added to the reaction mixture, and the incubation (with gentle shaking) was continued for additional hour at 4 °C. The bound Ras was then separated from the reaction mixture by passing the mixture through a glass fiber filter GF/B obtained from Millipore. The filter was washed three times with 2 mL of ice-cold washing buffer, and radioactivity on the filter was quantified by liquid scintillation counting. For the control, the above experiment was repeated, except that GST was used instead of GST-Raf. The data presented were the average of three independent experiments and fell within a range of 15%.

Fluorescence Measurement. Fluorescence emission of the H-*ras*-ANS complex was performed by titrating a constant amount of H-*ras* (complexed with either GDP or GTP) with 10−160 μM ANS as previously described (Crane & Miller, 1974). Fluorescence was measured in a Perkin-Elmer luminescence spectrometer (Model LS 50B) with an excitation wavelength of 350 nm (slit width 2.5 nm) and a detection wavelength of 440 nm (slit width 7.5 nm). The measurements were conducted at room temperature in a buffer containing 50 mM Tris-HCl, pH 7.4 and 5 mM $MgCl_2$. The concentration of H-*ras* was set at 2 μM. For each increment of dye concentration, the dye was allowed to bind to p21 for 2 min before measuring. At least ten readings were taken over a period of 2−3 min for each dye concentration. The readings were corrected for the background (dye only) before plotting.

Table 1: Apparent GDP/GTP Dissociation Constants of H-*ras* p21 Species

H-*ras* p21	K_D(GDP) (×10^{-8} M)	K_D(GTP) (×10^{-8} M)
v-H-*ras*	4.0	1.5
v-H-*ras*(G60A)	1.8	1.0

RESULTS

The Interaction of the G60A Mutant with GDP/GTP. H-*ras* proteins were expressed and purified as described in Materials and Methods. The apparent K_Ds for the GDP and GTP complexes of the wild type p21 and the G60A mutant were determined by equilibrium binding (Table 1). The apparent K_D indicates that the G60A mutant appears to have higher GDP/GTP binding affinity than v-H-*ras*. In agreement with these K_D values, v-H-*ras*(G60A) was found to exhibit a slower uncatalyzed GDP/GTP dissociation rate than the v-H-*ras* (Figure 1). Nevertheless, the difference is small and is unlikely to have much physiological significance. The uncatalyzed guanine nucleotide exchange rate was also determined, and again, we did not detect significant differences between v-H-*ras* and the G60A mutant (Figure 2). $G_{s\alpha}$-(G226A) exhibits a substantial GTP dissociation rate even at high Mg^{2+} concentrations compared to the wild type $G_{s\alpha}$

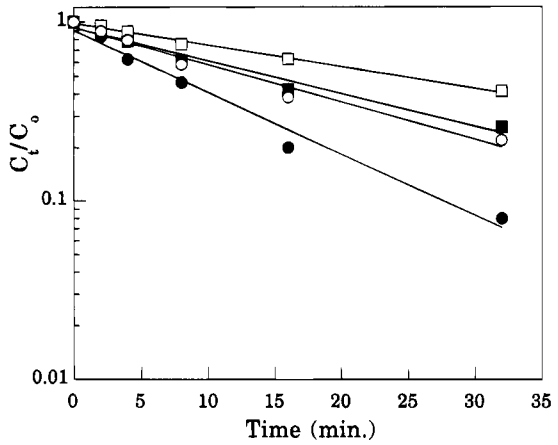

FIGURE 1: Intrinsic GDP/GTP dissociation of H-*ras* p21 species. GDP/GTP dissociation was measured by labeling p21 with [^{3}H]-GDP (● and ■) or [^{3}H]GTP (○ and □) to equilibrium, followed by chasing with a 500-fold excess of cold respective guanine nucleotides. The chase reactions were carried out in the presence of 0.5 mM free Mg^{2+} ion at 30 °C and quantified by the membrane filtration method. C_0 represents the amounts of GDP/GTP at time zero, and C_t represents the amounts of GDP/GTP at the indicated time point. v-H-*ras* (○ and ●) and v-H-*ras*(G60A) (□ and ■).

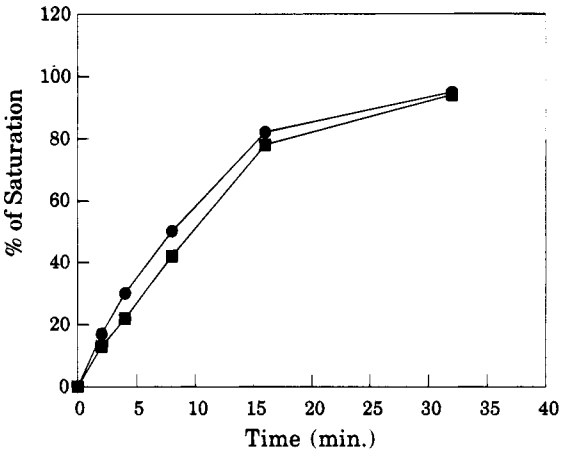

FIGURE 2: Intrinsic GDP exchange of H-*ras* p21 species. GDP exchange reactions were performed in the presence of 0.5 mM free Mg^{2+} ion as described in the Materials and Methods. v-H-*ras* (●) and v-H-*ras*(G60A) (■).

(Lee *et al.*, 1992); therefore, we performed GDP/GTP exchange and dissociation reactions at different concentrations of free Mg^{2+} ion ranging from 0 to 5 mM. The removal of Mg^{2+} ion gradually accelerates the rate of GDP/GTP exchange and release; however, rate enhancements were parallel in both v-H-*ras* and G60A mutant (data not shown), an observation contrasting to that of the $G_{s\alpha}$(G226A) mutant. Overall, our results indicate that the stability and kinetics of GDP/GTP binding of H-*ras* p21 are not significantly altered by the G60A mutation.

The Biological Activity of v-H-ras(G60A). NIH 3T3 cell transformation was used to measure the biological activity of wild type v-H-*ras* and the G60A mutant. Cells were transfected with pSV_{neo} vectors harboring these constructs, and the potency of transformation was scored as the number of foci formed. The result shows that the G60A mutation completely abolishes the transforming activity of v-H-*ras* (Table 2); its transforming activity is indistinguishable from that of the control vector or c-H-*ras*. Introducing viral or mutagenic H-*ras* p21 readily induces GVBD in *Xenopus* oocytes (Birchmeier *et al.*, 1985); thus, we also analyzed

Table 2: NIH 3T3 Cell Transforming Activity of H-*ras* p21 Species

H-*ras* p21	foci/μg of DNA
$pSV2_{neo}$, vector	0.1
c-H-*ras*	0.2
v-H-*ras*	123
v-H-*ras*(G60A)	0.1

Table 3: GVBD Induction in *Xenopus* Oocytes[a]

	% GVBD after		
injected material	12 h	18 h	24 h
buffer	0 (0/52)	0 (0/52)	0 (0/52)
c-H-*ras*	0 (0/55)	0 (0/55)	0 (0/55)
v-H-*ras*	38 (21/56)	79 (44/56)	100 (56/56)
v-H-*ras*(G60A)	0 (0/85)	0 (0/85)	0 (0/85)
v-H-*ras*(G60A)•GTP	0 (0/23)	0 (0/23)	0 (0/23)

[a] Oocyte injection was performed on oocytes obtained from four individual female frogs. The results were combined together. Numbers inside parentheses indicate the number of mature and total oocytes, respectively. Unless indicated otherwise, the amount of Ras p21 used for each oocyte was 46 ng.

the biological activity of purified H-*ras* p21 in *Xenopus* oocytes. Under our assay conditions, oocytes injected with 46 ng of v-H-*ras* mature within 24 h; while v-H-*ras*(G60A) is completely devoid of GVBD induction activity (Table 3). No GVBD was detected with injecting up to 92 ng of the G60A mutant and incubating up to 96 h (data not shown). In addition, prebinding GTP *in vitro* was unable to restore the GVBD induction activity to the G60A mutant (Table 3).

The Effects of G60A Mutation on SDC25C Interaction. SDC25C gene product from *Saccharomyces cerevisiae* is a H-*ras* p21 guanine nucleotide exchange factor (Crechet *et al.*, 1990; Mistou *et al.*, 1992; Hwang *et al.*, 1993). SDC25C enhances guanine nucleotide exchange by first displacing GDP from p21, forming an H-*ras* p21•SDC25C complex, and subsequently being displaced from the complex by GDP or GTP (Hwang *et al.*, 1993). The ability of the G60A mutant to form complexes with SDC25C under equilibrium conditions was analyzed in a gel-filtration column. H-*ras* p21 was labeled with [^{35}S]methionine *in vitro* and then used as a tracer for analysis. As shown in Figure 3A,B, v-H-*ras*(G60A) binds SDC25C and forms Ras•SDC25C to the same extent as the v-H-*ras*. With the addition of a 20-fold molar excess of SDC25C, approximately 35% of v-H-*ras* and 30% v-H-*ras*(G60A) were complexed. In addition, the amounts of GTP/GDP required for complex dissociation were also comparable; 0.2 μM GTP caused complete complex dissociation in both v-H-*ras* and the G60A mutant (Figure 3A,B). These results suggest that the G60A mutation does not alter p21's ability to interact with SDC25C. For comparison, H-*ras* harboring a guanine ring binding domain mutation, such as K117E, formed Ras•SDC25C complexes in much higher yield, and it required much higher concentrations of GDP/GTP to dissociate the complex (Figure 3C) (Hwang *et al.*, 1993). The steady-state kinetic study revealed that the apparent K_ms of SDC25C-stimulated guanine nucleotide exchange for the wild type and the G60A mutant were similar (Table 4), a result in accord with the equilibrium SDC25C binding. However, the rate of SDC25C-stimulated exchange was reduced by the G60A mutation (Figure 4). We found that the G60A mutation lowered the k_{cat} of

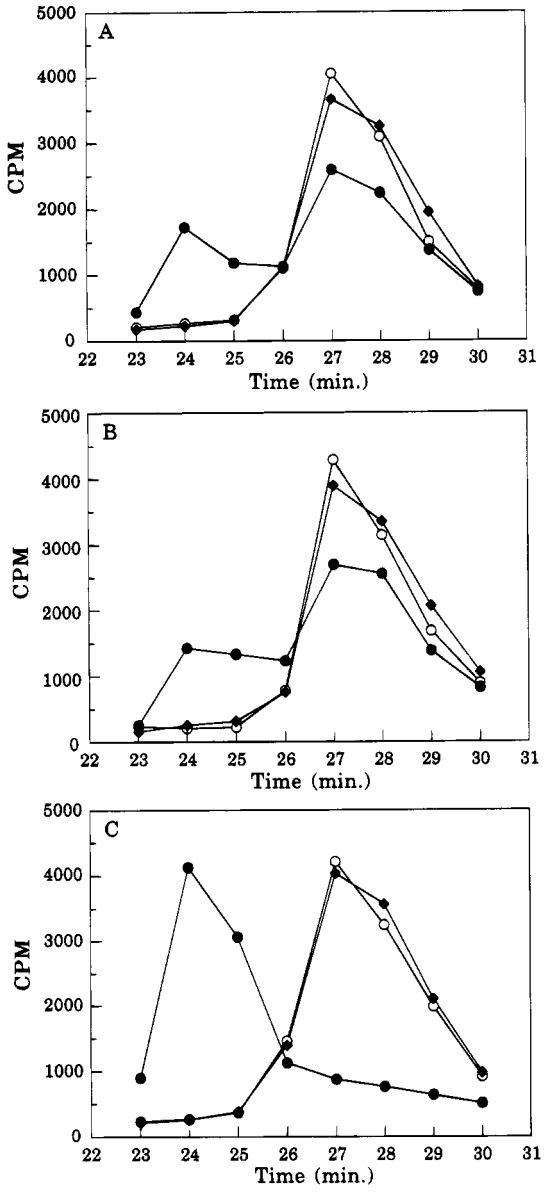

FIGURE 3: Interaction of H-*ras* species with SDC25C and GTP. Experiments were performed by mixing approximately 0.2 pmol of labeled H-*ras* with either 26 pmol (A and B) or 13 pmol (C) of SDC25C followed by elution in a Superdex 75 HR column. (A) v-H-*ras* control (○), v-H-*ras* plus SDC25C (●), and v-H-*ras* plus SDC25C in the presence of 0.2 μM GTP (♦). (B) v-H-*ras*(G60A) control (○), v-H-*ras*(G60A) plus SDC25C (●), and v-H-*ras*(G60A) plus SDC25C in the presence of 0.2 μM GTP (♦). (C) v-H-*ras*(K117E) control (○), v-H-*ras*(K117E) plus SDC25C (●), and v-H-*ras*(K117E) plus SDC25C in the presence of 0.1 mM GTP (♦).

Table 4: Apparent Kinetic Parameters of SDC25C-Stimulated Guanine Nucleotide Exchange

H-*ras* p21	K_m (μM)	k_{cat} (min^{-1})
v-H-*ras*	2.2	7.40
v-H-*ras*(G60A)	3.1	1.45

SDC25C-stimulated GDP exchange by about 5-fold (Table 4).

The Effects of G60A Mutation on GAP Interaction. The v-H-*ras* exhibits very low intrinsic and GAP-stimulated GTPase activities; thus, a competition method (Vogel *et al.*, 1988) rather than the direct GTP hydrolysis measurement was employed to analyze the interaction of Ras and GAP.

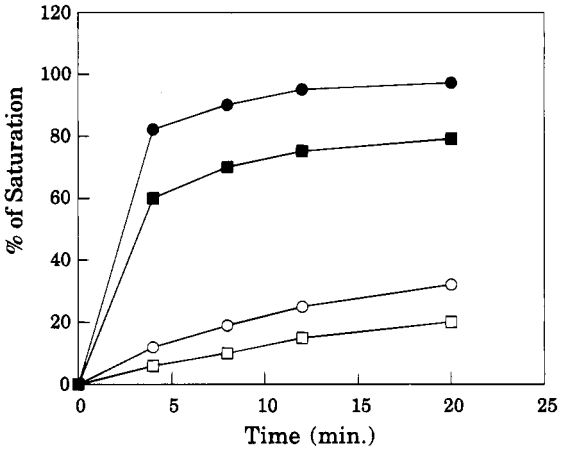

FIGURE 4: GDP exchange of v-H-*ras* and v-H-*ras*(G60A) stimulated by SDC25C. SDC25C-stimulated GDP exchange was performed in the presence of 2 mM free Mg^{2+} ion as described in the Materials and Methods. v-H-*ras* control (○), v-H-*ras*(G60A) control (□), v-H-*ras* plus SDC25C (●), and v-H-*ras*(G60A) plus SDC25C (■).

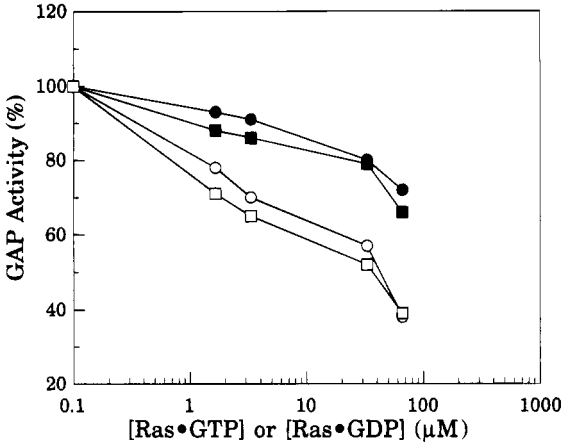

FIGURE 5: Inhibition of GAP activity by v-H-*ras* and v-H-*ras*(G60A). The experiments were performed by measuring the GAP-stimulated GTP hydrolysis of c-H-*ras*•[γ-^{32}P]GTP in the presence of indicated amounts of competitor H-*ras* p21. Constant amounts of full-length human GAP (2.8 nM) were used throughout the experiments. Competing H-*ras* species were v-H-*ras*•GDP (●), v-H-*ras*(G60A)•GDP (■), v-H-*ras*•GTP (○), and v-H-*ras*(G60A)•GTP (□).

Ras in its GTP-bound state is able to compete against other Ras molecules for GAP and cause an apparent reduction in GAP activity. This reduction in GAP activity can be used as an indicator for assessing the p21 and GAP interactions (Vogel *et al.*, 1988). Thus, we measured the strength of the GAP-inhibiting ability of wild type v-H-*ras*•GTP and v-H-*ras*(G60A)•GTP. As shown in Figure 5, v-H-*ras*(G60A)•GTP displays slightly higher inhibitory activity against GAP than v-H-*ras*•GTP over a range of competitor concentrations. This observation suggests that v-H-*ras*(G60A) has a higher affinity for GAP than the wild type v-H-*ras*. The GDP-bound forms of v-H-*ras* and v-H-*ras*(G60A) were used as controls, and both were less effective than the GTP-bound form in reducing GAP activity (Figure 5). The steady-state inhibition constants of v-H-*ras*•GTP and v-H-*ras*(G60A)•GTP in the GAP-stimulated reaction were determined to be 69 μM for v-H-*ras*•GTP and 51 μM for v-H-*ras*(G60A)•GTP at a GAP concentration of 2.8 nM. Again, the G60A mutation was found to enhance the binding of H-*ras* p21 to GAP; however,

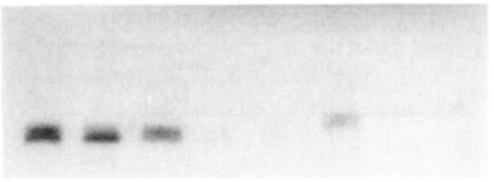

FIGURE 6: The interaction of Ras and Raf. The coprecipitation of [^{35}S]-labeled Ras and GST-Raf by glutathione−Sepharose was performed in the presence of the following components: lane 3, v-H-*ras*•GTP plus GST-Raf; lane 4, v-H-*ras*•GTP plus GST; lane 5, v-H-*ras*•GDP plus GST-Raf; lane 6, v-H-*ras*(G60A)•GTP plus GST-Raf; lane 7, v-H-*ras*(G60A) plus GST; and lane 8, v-H-*ras*(G60A)•GDP plus GST-Raf. The starting materials for precipitation, v-H-*ras*•GTP and v-H-*ras*(G60A)•GTP, were shown in lanes 1 and 2, respectively.

Table 5: Analysis of Ras and Raf Interaction by Coprecipitation

H-*ras* p21	% of Ras coprecipitated by GST	% of Ras coprecipitated by GST-Raf
[^{35}S]-v-H-*ras*•GTP	<0.1	10.9
[^{35}S]-v-H-*ras*•GDP	ND[a]	<0.1
[^{35}S]-v-H-*ras*(G60A)•GTP	0.1	3.4
[^{35}S]-v-H-*ras*(G60A)•GDP	ND	0.9
v-H-*ras*•[^{32}P]-GTP	1.3	24.6
v-H-*ras*(G60A)•[^{32}P]-GTP	1.1	8.3

[a] ND: not determined.

the difference may be negligible under physiological conditions. Overall, we conclude that G60A mutation does not affect the interaction of Ras and GAP.

The Effects of G60A Mutation on Raf Interaction. We subsequently examined the ability of H-ras(G60A) to interact with Raf protein, the putative Ras effector which binds Ras in a GTP-dependent manner (Van Aslet *et al.*, 1993; Vojtek *et al.*, 1993; Warne *et al.*, 1993; Zhang *et al.*, 1993). A GST fusion clone containing the N-terminal 275 residues of Raf protein (including the Ras binding domain) was used in the assay. Briefly, GST-Raf was allowed to interact with [^{35}S]-methionine-labeled Ras•GTP, and then the complexes were coprecipitated using glutathione−Sepharose gel. The coprecipitated [^{35}S]-labeled Ras was then analyzed and quantified. As expected, the Ras-Raf interaction is GTP-dependent as GTP greatly enhances Raf binding activity of Ras (Figure 6 and Table 5). We found that about 10.9% v-H-*ras*•GTP but less than 0.1% v-H-*ras*•GDP were coprecipitated. In contrast, about 3.4% v-H-*ras*(G60A)•GTP was coprecipitated, a value which is about 3-fold lower than that of v-H-*ras* (Figure 6 and Table 5). The Raf binding of the G60A mutant still exhibited GTP dependence; that is, v-H-*ras*(G60A)•GDP was substantially greater than v-H-*ras*•GDP (Table 5). Alternatively, we also measured Ras-Raf binding by coprecipitation of GST-Raf and purified Ras p21 complexed with [γ-^{32}P]GTP. The result of the [^{32}P]-labeled experiment was essentially the same as that of the preceding experiment, which showed that Raf binding activity of v-H-*ras* was reduced approximately 3-fold by the G60A mutation (Table 5). It should be noted that Zn^{+2} ion was found to be absolutely essential for the Ras-Raf interaction in our assay.

The Effects of G60A Mutation on the GTP-Induced Fluorescence Enhancement of H-ras and ANS Complex. The fluorescence dye ANS has been used to distinguish GTP- and GDP-bound forms of EF-Tu. In that study, EF-Tu•GTP

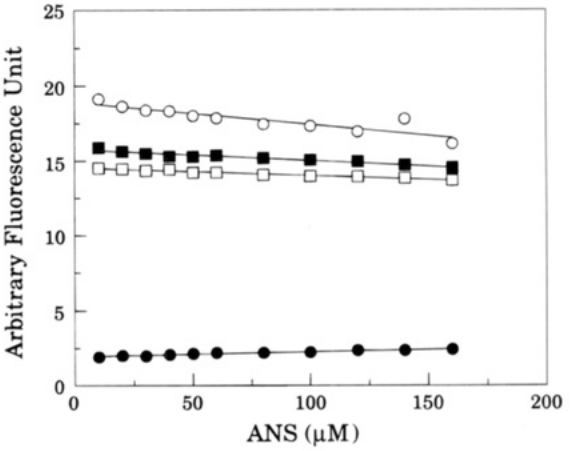

FIGURE 7: Fluorescence emission of Ras•guanine nucleotide•ANS ternary complex. The ANS titration experiment was performed as described in the Materials and Methods. The scale used in the plot was an arbitrary fluorescence unit. Symbols used in the figure are v-H-*ras*•GDP (●), v-H-*ras*(G60A)•GDP (■), v-H-*ras*•GTP (○), and v-H-*ras*(G60A)•GTP (□).

was found to enhance the fluorescence of ANS to a greater extent than EF-Tu•GDP (Crane & Miller, 1974). We adapted the method to probe different conformations of p21. Similar to EF-Tu, the addition of H-*ras* causes a blue shift in the wavelength of maximum dye emission from approximately 500 to 440 nm (data not shown), and the intensity of emission around 440 nm is guanine nucleotide-dependent. Compared to GDP, GTP binding greatly enhances fluorescence emission around this wavelength; therefore, we measured the fluorescence emission of GTP- and GDP-bound p21 at 440 nm. GTP-bound v-H-*ras* produced a fluorescence emission which was about 9-fold greater than that of GDP-bound v-H-*ras*, and the enhancement persisted over a wide range of ANS concentrations (10−160 μM). In contrast to v-H-*ras*, the G60A mutant did not exhibit an emission enhancement induced by GTP (Figure 7), a result suggesting that the GTP- and the GDP-bound forms of the G60A mutant possess similar conformations. Nevertheless, the G60A mutant displays an emission intensity which is much closer to that of the v-H-*ras*•GTP form than that of the v-H-*ras*•GDP form (Figure 7).

DISCUSSION

The X-ray structures of regulatory GTPases indicate that these proteins utilize the Gly residue (Gly-60 in H-*ras* p21) of the DXXG motif as a hinge for GTP-induced conformational changes. This residue reorients in response to GTP and forms a direct bond with the γ-phosphate. This event subsequently triggers a larger scale molecular rearrangement and allows the protein to assume a proper conformation for target interaction and GTP hydrolysis (Pai *et al.*, 1990; Milburn *et al.*, 1990; Berchtold *et al.*, 1993; Kjeldgaard *et al.*, 1993; Noel *et al.*, 1993; Lambright *et al.*, 1994). Glycine is uniquely suitable for this structural role because it exhibits a much broader range of ϕ and ψ dihedral angles than other amino acids (Richardson, 1981). Accordingly, these models imply that GTP-induced activities, such as effector interactions or GTP hydrolysis, may be impaired if the Gly residue is substituted by other amino acids. This hypothesis has been confirmed by the study of $G_{s\alpha}$(G226A) and EF-Tu(G83A) mutants (Miller *et al.*, 1988; Lee *et al.*, 1992; Hwang *et al.*, 1989).

We constructed and examined v-H-*ras* harboring the G60A mutation, a mutation corresponding to $G_{s\alpha}$(G226A) and EF-Tu(G83A). Although the G60A mutation has little or no effect on the GDP/GTP binding, intrinsic GDP/GTP exchange and dissociation, it completely abolishes the ability of v-H-*ras* to transform NIH 3T3 cells and to induce GVBD in *Xenopus* oocytes. This observation is consistent with the finding that the Gly-60 to Asp mutation of H-*ras* is inactive in yeast (Mosteller *et al.*, 1994). There is no significant difference between the wild type and the G60A mutant in their interaction with GDP/GTP; therefore, it is unlikely that the defect in the biological activity associated with the G60A mutation can be attributed to structural perturbation at the GDP/GTP binding site. The lack of biological activity also cannot be attributed to the failure of v-H-*ras*(G60A) to exchange GDP for GTP because prebinding GTP to v-H-*ras*(G60A) did not restore the GVBD induction activity in the oocyte injection assay. In addition, the interaction of the G60A mutant with one of the guanine nucleotide exchange factors, SDC25C, appears to be normal (see below). Gly-60 itself is unlikely to directly participate in effector interaction; therefore, in light of the studies of $G_{s\alpha}$-(G226A) and EF-Tu(G83A) (Miller *et al.*, 1988; Lee *et al.*, 1992; Hwang *et al.*, 1989), we postulate that the G60A mutation eliminates the biological activity of v-H-*ras* by preventing the GTP-bound H-*ras* p21 from switching into the active conformation. This postulate is supported by our observations.

The interaction of H-*ras* p21 with SDC25C was not altered by the G60A mutation under both steady-state and equilibrium conditions. The K_ms of the SDC25C-stimulated reactions for the wild type and the G60A mutant were essentially the same, and we did not detect a significant difference between the wild type and the G60A mutant in forming H-*ras*•SDC25C complexes. This result establishes that Gly-60 of H-*ras* is not part of SDC25C binding domain. Nevertheless, the guanine nucleotide exchange promoted by SDC25C was notably decreased by the mutation. This result is consistent with earlier findings that mutation at residues around Gly-60, such as at positions 61, 62, and 63, changes the rate but not the K_m of the SDC25C-stimulated reaction (Mistou *et al.*, 1992). Because these residues are either close to or at the GDP/GTP binding pocket, the reduction in the rate of guanine nucleotide exchange is not surprising.

Interestingly, the G60A mutation reduces the binding of Ras to Raf but not to GAP (Figures 5 and 6 and Table 5). Although both require the GTP form of H-*ras* to bind, our observation suggests that the GAP and Raf binding sites do not completely overlap. The ability to differentiate Raf from GAP offers a possibility that one may be able to determine the essential core structure of GAP and Raf binding sites using the G60A mutant. The G60A mutant still possesses Raf binding activity. If the sole function of H-*ras* p21 is to recruit Raf to the membrane as suggested by recent reports (Leevers *et al.*, 1994; Stokoe *et al.*, 1994), one would expect that the G60A mutant would exhibit some biological activity. Apparently, this is not the case (Tables 2 and 3). We cannot explain why the G60A mutant is completely devoid of biological activity based on the Raf binding activity; nevertheless, we should point out that a previous attempt of trying to match the Raf binding and transforming ability also failed to establish a perfect correlation (Chuang *et al.*, 1994).

The GTP-induced conformational change of H-*ras* p21 was examined by the fluorescence dye ANS. ANS has been used successfully to probe the structural differences between the GDP- and GTP-bound forms of EF-Tu (Crane & Miller, 1974). GTP enhances the fluorescence emission of the EF-Tu•ANS complex by permitting more ANS binding to EF-Tu. Similar to EF-Tu, the fluorescence emission of the H-*ras*•ANS complex is also enhanced by GTP (Figure 7). The increase in emission intensity may be due to either more ANS binding or a higher quantum yield. Our current data are unable to distinguish these two possibilities. The enhancement of fluorescence emission was found to be completely abolished by the G60A mutation (Figure 7). This observation offers direct evidence to support the hypothesis that GTP-induced conformational change is impaired in the G60A mutant. Despite the fact that it does not possess a GTP-induced emission enhancement, the G60A mutant (either GDP or GTP form) consistently displays a much higher emission intensity than H-*ras*•GDP. The mechanism of this observation is not clear. It may be that the G60A mutant is locked in a structure which allows either more ANS binding or higher quantum yield. Apparently, the structure of H-*ras*(G60A) is different from that of H-*ras*•GDP or H-*ras*•GTP.

GTP induces conformational changes, primarily, in two regions of H-*ras* p21, residues 30−38 (switch I) and residues 60−76 (switch II). Since the G60A mutation blocks GTP-induced activities, it is likely that switches I and II are candidates for the G60A mutation effect. We should point out that while the GTP-enhanced ANS emission is blocked by the G60A mutation (Figure 7), the GAP binding and to some extent the Raf binding activity of the G60A mutant still exhibit GTP dependence (Figures 5 and 6). Therefore, it is clear that not every aspect of the GTP-induced conformational change is abolished by the G60A mutation.

In its GTP-bound state, $G_{s\alpha}$ resists cleavage by trypsin at Arg-232 (Miller *et al.*, 1988; Lee *et al.*, 1992), while both the GDP-bound $G_{s\alpha}$ and the GTP-bound form of $G_{s\alpha}$(G226A) are trypsin-sensitive. This result suggests that the region at or near Arg-232 of $G_{s\alpha}$ (the corresponding region of switch II) cannot assume its activated (and trypsin-resistant) conformation when Gly-226 is mutated (Miller *et al.*, 1988; Lee *et al.*, 1992). This conclusion is further strengthened by the observation that the GTP-dependent intrinsic fluorescence of Trp-234 is eliminated by the G226A mutation (Lee *et al.*, 1992). In EF-Tu, GTP binding accelerates the rate of trypsin cleavage at Arg-59 (Douglass & Blumenthal, 1979); however, this rate was not altered by the G83A mutation (Hwang *et al.*, 1989). This result suggests that the G83A mutation does not affect the GTP-induced conformational changes at or near Arg-59 of EF-Tu, a region corresponding to the switch I domain (Bourne *et al.*, 1990, 1991; Berchtold *et al.*, 1993; Kjeldgaard *et al.*, 1993). At present, we do not know which switch region is affected by the G60A mutation. Nevertheless, through the findings of $G_{s\alpha}$(G226A) and EF-Tu(G83A), it appears that the failure of switch II to rearrange may be the key consequence of the G60A mutation. If this speculation is correct, it implies that the binding of Raf requires the cooperation of two switch regions, while the binding of GAP may only need switch region I (effector domain). Since the G60A mutation eliminates the biological activity of v-H-*ras* p21, it also implies that the switch II region is one of the essential domains for the biological

function of v-H-*ras* p21. Our speculation is supported by the mutagenesis study at Tyr-64 of H-*ras* (Nur-E-Kamal *et al.*, 1992); however, it is in direct contrast to the finding that part of the switch II region can be deleted without affecting the biological activity of v-H-*ras* (Willumsen *et al.*, 1986). In contrast to the Ras and SDC25C interaction, the interaction of Ras with the CDC25 gene product is altered by mutation in the region of residues 62−69 (Mosteller *et al.*, 1994). Our conclusion implies that the G60A mutation may affect the interaction of Ras with CDC25 or other guanine nucleotide exchange factors. This possibility is currently under study.

Heterotrimeric G-proteins, EF-Tu, and H-*ras* p21 appear to share a fundamental molecular mechanism for GTP-induced conformation changes, a mechanism that may be generally conserved in all other regulatory GTPases. Since each protein interacts with different cellular components and performs different functions, such a mechanism has evolved into different formats. For example, similar conformational changes are required for dissociation of α from $\beta\gamma$ subunits in heterotrimeric G-proteins, for the binding of aminoacyl-tRNA binding in EF-Tu, and for GAP and Raf interaction in H-*ras* p21. Because the G60A mutation is able to prevent the GTP-induced conformational change and distinguish between GAP and Raf, it will provide a useful tool for elucidating the molecular mechanism of GTP-induced conformational change and effector interaction.

ACKNOWLEDGMENT

We thank Drs. Frank McCormick and Gideon Bollag of Onyx Pharmaceuticals for providing Ras GAP, Andrea Parmeggiani for supplying SDC25C, Ulf R. Rapp for the Raf clone, Thomas Y. Shih for conducting the NIH 3T3 cell transformation, and Diwakar Dushmukh for providing luminescence spectrometer. We also thank Drs. Robert Denman, Carl Dobkin, and David Miller for critical reading of the manuscript.

REFERENCES

Berchtold, H., Reshetnikova, L., Reiser, C. O., Schirmer, N. K., Sprinzl, M., & Hilgenfeld, R. (1993) *Nature 365*, 126−132.

Birchmeier, C., Broek, D., & Wigler, M. (1985) *Cell 43*, 615−621.

Bollag, G., & McCormick, F. (1991) *Annu. Rev. Cell Biol. 7*, 601−632.

Bonner, T. I., Oppermann, H., Seeburg, P., Kerby, S. B., Gunnell, M. A., Young, A. C., & Rapp, U. R. (1986) *Nucleic Acids Res. 14*, 1009−1015.

Bourne, H. R., Sanders, D. A., & McCormick, F. (1990) *Nature 348*, 125−132.

Bourne, H. R., Sanders, D. A., & McCormick, F. (1991) *Nature 349*, 117−127.

Chuang, E., Barnard, D., Hettich, L., Zhang, X. F., Avruch, J., & Marshall, M. S. (1994) *Mol. Cell Biol. 14*, 5318−5325.

Crane, L. J., & Miller, D. L. (1974) *Biochemistry 13*, 933−939.

Crechet, J.-B., Poullet, P., Mistou, M.-Y., Parmeggiani, A., Camonis, J., Boy-Marcotte, E., Damak, F., & Jacquet, M. (1990) *Science 248*, 866−868.

Crystal, R. G., Elson, N. A., & Anderson, W. F. (1974) *Methods Enzymol. 30*, 101−127.

Dever, T. E., Glynias, M. J., & Merrick, W. C. (1987) *Proc. Natl. Acad. Sci. U.S.A. 84*, 1814−1818.

De Vos, A. M., Tong, L., Milburn, M. V., Matias, P. M., Jancarik, J., Noguchi, S., Nishimura, S., Miura, K., Ohtsuka, E., & Kim, S.-H. (1988) *Science 239*, 888−893.

Douglass, J., & Blumenthal, T. (1979) *J. Biol. Chem. 254*, 5383−5387.

Dumont, J. (1972) *J. Morphol. 136*, 153−180.

Gilman, A. G. (1987) *Annu. Rev. Biochem. 56*, 615−649.

Gurdon, J. B., Fairman, S., Mohun, T. J., & Brennan, S. (1985) *Cell 41*, 913−922.

Hwang, Y. W., Jurnak, F., & Miller, D. L. (1989) in *The guanine-nucleotide binding proteins, common structural and functional properties* (Bosch, L., Kraal, B., & Parmeggiani, A., Eds.) pp 77−85, Plenum Press, New York.

Hwang, Y. W., Zhong, J. M., Poullet, P., & Parmeggiani, A. (1993) *J. Biol. Chem. 268*, 24692−24698.

Jurnak, F. (1985) *Science 230*, 32−36.

Jurnak, F., Heffron, S., & Bergmann, E. (1990) *Cell 60*, 525−528.

Kjeldgaard, M., Nissen, P., Thirup, S., & Nyborg, J. (1993) *Structure 1*, 35−50.

Kunkel, T. A., Roberts, J. D., & Zakour, R. A. (1987) *Methods Enzymol. 154*, 367−382.

la Cour, T. F. M., Nyborg, J., Thirup, J., & Clark, B. F. C. (1985) *EMBO J. 4*, 2385−2388.

Lambright, D. G., Noel, J. P., Hamm, H. E., & Sigler, P. B. (1994) *Nature 369*, 621−628.

Lee, E., Taussig, R., & Gilman, A. G. (1992) *J. Biol. Chem. 267*, 1212−1218.

Leevers, S. J., Paterson, H. F., & Marshall, C. J. (1994) *Nature 369*, 411−414.

Manne, V., Yamazaki, S., & Kung, H.-F. (1984) *Proc. Natl. Acad. Sci. U.S.A. 81*, 6953−6957.

Marshall, M. S. (1993) *Trends Biochem. Sci. 18*, 250−254.

Milburn, M. V., Tong, L., De Vos, A. M., Brunger, A., Yamaizumi, Z., Nishimura, S., & Kim, S.-H. (1990) *Science 247*, 939−945.

Miller, D. L., & Weissbach, H. (1974) *Methods Enzymol. 30*, 219−232.

Miller, R. T., Masters, S. B., Sullivan, K. A., Beiderman, B., & Bourne, H. R. (1988) *Nature 334*, 712−715.

Mistou, M. Y., Jacquet, E., Poullet, P., Rensland, H., Gideon, P., Schlichting, I., Wittinghofer, A., & Parmeggiani, A. (1992) *EMBO J. 11*, 2391−2397.

Moodie, S. A., Willumsen, B. M., Weber, M. J., & Wolfman, A. (1993) *Science 260*, 1588−1590.

Mosteller, R. D., Han, J., & Broek, D. (1994) *Mol. Cell Biol. 14*, 1104−1112.

Noel, J. P., Hamm, H. E., & Sigler, P. B. (1993) *Nature 366*, 654−663.

Nur-E-Kamal, M. S. A., Sizeland, A., D'abaco, G., & Maruta, H. (1992) *J. Biol. Chem. 267*, 1415−1418.

Ogiso, Y., Gutierrez, L., Wrathall, L. S., Lu, Y.-Y., Blair, D. G., Clanton, D. J., Hwang, Y. W., & Shih, T. Y. (1990) *Cell Growth Differ. 1*, 217−224.

Pai, E. F., Kabsch, W., Krengel, U., Holmes, K. C., John, J., & Wittinghofer, A. (1989) *Nature 341*, 209−214.

Pai, E. F., Krengal, U., Petsko, G. A., Goody, R. S., Kabsch, W., & Wittinghofer, A. (1990) *EMBO J. 9*, 2351−2359.

Richardson, J. S. (1981) *Adv. Protein Chem. 34*, 167−339.

Stokoe, D., Macdonald, S. G., Cadwallader, K., Symons, M., & Hancock, J. F. (1994) *Science 264*, 1463−1467.

Stouten, P. F. W., Sander, C., Wittinghofer, A., & Valencia, A. (1993) *FEBS Lett. 320*, 1−6.

Valencia, A., Kjeldgaard, M., Pai, E. F., & Sanders, C. (1991) *Proc. Natl. Acad. Sci. U.S.A. 88*, 5443−5447.

Van Aslet, L., Barr, M., Marcus, S., Polverino, A., & Wigler, M. (1993) *Proc. Natl. Acad. Sci. U.S.A. 90*, 6213−6217.

Vogel, U. S., Dixon, R. A. F., Schaber, M. D., Diehl, R. E., Marshall, M. S., Scolnick, E. M., Sigal, I. S., & Gibbs, J. B. (1988) *Nature 335*, 90−93.

Vojtek, A. B., Hollenberg, S. M., & Cooper, J. A. (1993) *Cell 74*, 205−214.

Warne, P. H., Viciana, P. R., & Downward, J. (1993) *Nature 364*, 352−355.

Willumsen, B. M., Papageorge, A. G., Kung, H.-F., Bekesi, E., Robins, T., Johnsen, M., Vass, W. C., & Lowy, D. R. (1986) *Mol. Cell Biol. 6*, 2646−2654.

Zhang, X. F., Settleman, J., Kyriakis, J. M., Takeuchi-Suzuki, E., Elledge, S. J., Marshall, M. S., Bruder, J. T., Rapp, U. R., & Avruch, J. (1993) *Nature 364*, 308−313.

BI942343D